ISSN: 2093-5374 / E-ISSN: 2093-5382

Efficient Monte Carlo Algorithms based on Stochastic Geometry for Simulating Downlink and Uplink Cellular Communications

Gehad Taher[1*], El-Sayed El-Hady[2], and Hamed Nassar[3]

[1*]Computer Science Department, Suez Canal University, Ismailia, Egypt.
gehad.Taher@ci.suez.edu.eg, https://orcid.org/0000-0002-0066-4734

[2]Basic Sciences Department, Suez Canal University, Ismailia, Egypt.
elsayed _elhady@ci.suez.edu.eg, https://orcid.org/0000-0002-4955-0842

[3]Computer Science Department, Suez Canal University, Ismailia, Egypt.
nassar@ci.suez.edu.eg, https://orcid.org/0000-0001-8528-5102

Received: March 04, 2024; Revised: May 20, 2024; Accepted: July 04, 2024; Published: September 30, 2024

Abstract

Stochastic geometry (SG) is increasingly utilized in modeling cellular communications systems, as it yields accurate and realistic analytical results. The most common aim of such modeling is to characterize the coverage probability in both the downlink (DL) and uplink (UL) directions. To validate these results, however, researchers need to use simulation, for which efficient algorithms are by and large not available, and that is where the present article comes in. We introduce here two SG based Monte Carlo algorithms to simulate DL and UL cellular communications efficiently and accurately. The algorithms are so comprehensive that they take the parameters of the system as input and deliver its coverage probability as output, considering in the process such details as equipment deployment, signal power, interference, and channel conditions. To demonstrate their superior efficiency, the algorithms have been analyzed rigorously. To test their accuracy, they have been coded and applied to some sample systems, producing results that match those produced analytically to within 4% in DL and 5% in UL. Although they are designed for the field of communications, the algorithms can be easily adapted for other fields where SG is also applicable, such as biology, astronomy and forestry.

Keywords: Cellular Network Deployment, IoT, Simulation Algorithm, Stochastic Geometry, Downlink/Uplink Coverage Probability.

1 Introduction

Stochastic geometry (SG) was initially stimulated by applications in biology, astronomy and material sciences, then introduced seriously in the late nineties to the field of wireless communications (Okegbile et al., 2021). It is particularly suited for modeling large scale wireless networks, where a network is treated as a realization (snapshot) of a spatial point process in the entire Euclidean plane, as shown in Figure 1. Accordingly, it well describes node locations in randomly formed networks such as cellular and ad-hoc networks. It also provides a smooth way of computing macroscopic properties, by averaging over the spatial patterns of the network nodes to obtain important performance characteristics, e.g.

Journal of Wireless Mobile Networks, Ubiquitous Computing, and Dependable Applications (JoWUA), volume: 15, number: 3 (September), pp. 1-16. DOI: *10.58346/JOWUA.2024.I3.001*

*Corresponding author: Computer Science Department, Suez Canal University, Ismailia, Egypt.

connectivity, stability, and coverage probability. The spatial averaging afforded by SG is a key paradigm shift in communications systems performance evaluation, where temporal averages were dominant. Further, SG results are typically functions of a relatively small number of parameters, e.g. intensity of the underlying point process and the channel conditions.

In cellular communications, the most common use of SG is to characterize the signal to interference and noise ratio (SINR) (Priyanka et al., 2023; Amira et al., 2023). This metric is important as it can be used to calculate many performance metrics, such as the coverage probability, channel throughput and spectral efficiency (Okegbile et al., 2021). It is worth mentioning, however, that due to the huge amount of wireless emissions nowadays, the contribution of noise to the ratio can be considered zero (Liu et al., 2019). Under such interference limited conditions, there is a growing modeling trend (see, for example, Nidhi et al., 2024; Liu & Zhang, 2020); Naga et al., 2024; Tang et al., 2020; Kouzayha et al., 2021) to replace SINR by SIR, and we will follow this trend in the present article.

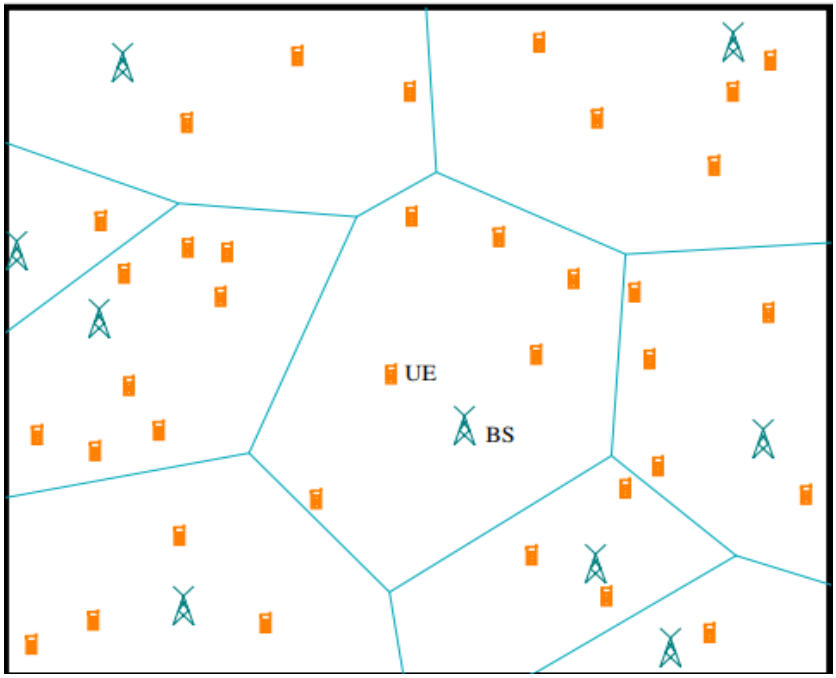

Figure 1: A Poisson-Voronoi Tessellation Model of a Cellular Network. The BSs, induced by a PPP, partition the Euclidean plane into Voronoi cells, each having one BS and a number of UEs, with the property that a UE in any cell is closer to the BS of that cell than to any other BS in the plane. This tessellation is so natural and realistic for cellular networks that it has superseded the once popular grid of hexagonal cells

In SG modeling of cellular networks, base stations (BS) can be represented by any one of many point processes, such as Thomas cluster process, Matérn cluster process, and Poisson Point Process (PPP) (Błaszczyszyn et al., 2018). The last is the most common (Masato et al., 2024; Björnson et al., 2016) and is also the one used in the present article. With the BSs deployed as a PPP, each user equipment (UE) will associate itself with the closest BS, making the plane take the shape of the Poisson-Voronoi tessellation shown in Figure 1. This tessellation has proved a more accurate alternative to the once popular hexagonal grid tessellation (Błaszczyszyn et al., 2018).

An important cellular communications technique, considered in the present article, is fractional power control (FPC), whereby each UE adjusts its power level in the UL direction under the control of

the serving BS. More specifically, each UE controls its transmit power such that the received signal power at its serving BS is equal to a predefined threshold. This control benefits both the UE, by saving its energy, and the BS, by increasing the SIR there. In general, the optimal levels of transmit power in a network depend on path loss, shadowing, and multipath fading, as well as the network configuration.

Our motive for the present article is that we have not spotted any formal simulation algorithms for SG models of cellular communications, although countless studies of the same abound. After diligent search, what could be found is only code; but even that is rare, haphazard and poorly documented. Our contribution in the present article is intended to fill this gap. Specifically, we present two efficient simulation algorithms whose results impressively match those obtained analytically.

Contribution: The contribution of this article is two efficient SG-based, Monte Carlo-type algorithms to simulate cellular communications in both the DL and UL directions. No such algorithms have ever been published before, to the best of our knowledge, despite their paramount importance in validating theoretical work in the wireless communications field. What is more, they can also be easily adapted for other fields which also use SG models, such as material science, biology, forestry and astronomy.

The rest of the article is organized as follows. Section 2 reviews some SG models of cellular networks published recently in the literature. Section 3 presents the particular model that we are going to simulate, and in Section 4 we introduce the proposed simulation algorithms for that model. Numerical results for some sample systems are presented in Section 5. Section 6 has the conclusions.

2 Related Work

The real momentum of using SG as a modeling vehicle for wireless systems, especially cellular networks, has been gained over the past decade (Siddiquee et al., 2018; Megías et al., 2022). A huge body of research in this area has been carried out, which can be categorized according to the direction of transmission, i.e. DL, UL or both.

Extensive work has focused on DL modeling under different scenarios, such as lognormal shadowed fading (Chen & Yuan, 2019), queueing delay (Liu et al., 2020), ultra-dense deployment, where there are lots of low power small SBSs overlapping macro BSs (Liu & Zhang, 2020). Examples of the last include HetNets with *K*-tiers (Fadoul, 2020), ultradense HetNets (Lei et al., 2018; Fadoul, 2020), and decoupled HetNets (Llopiz-Guerra et al., 2024; Arif et al., 2020).

Equally extensive work has focused on UL modeling for different scenarios, such as wake-up signals for Internet of Things (IoT) applications (Kouzayha et al., 2017), dense deployment (Nur et al., 2023; Li et al., 2024), interference limitedness (Liu et al., 2019), independent distribution of BSs and UEs (Talić & Mešić, 2022; Mariam et al., 2021) truncated FPC control (Kamiya et al., 2020), composite Rayleighlognormal fading (Herath et al., 2018), millimeter wave HetNets (Onireti et al., 2020), decoupled UL and DL association (DUDA) (Jia et al., 2019), and decoupled dense HetNet (Ali et al., 2019).

In addition, there is much work that focuses on both DL and UL, under different conditions, such as massive multiple-input multiple-output (M-MIMO) (Sadeghabadi et al., 2019), unmanned aerial vehicle (UAV)-assisted cellular networks (Wang & Gursoy, 2019; Liu & Zhang, 2020), and cell association based on DL signal power (Bouras & Kalogeropoulos, 2020).

Research Gap: Despite the existence of a huge body of research work on SG modelling of cellular communications, we have not found any work on the SG simulation of cellular communications. Upon

diligent search in the literature, no SG simulation algorithms have ever been presented, let alone analyzed. The present work is intended to fill this gap.

3 Model

The key aspect of the model discussed in the present work is that the BSs are deployed according to a PPP Φ. This means they are randomly scattered in the Euclidean plane with independent locations.

We denote the distance between the associated BS-UE pair throughout by *R*. In addition, each transmitter, whether BS or UE, on an active communications channel uses a nominal transmit power of $\mathfrak{p}$.

We consider cell orthogonal communications. This implies that in each cell only one UE can be active, communicating with the BS of that cell, on any time/frequency resource. Accordingly, Figure 2 is a snapshot of all the active devices, in all the cells, that are currently communicating on the same frequency. Since every BS-UE pair in the Figure operates on the same resource, there is inter-cell interference which we will characterize below.

Before proceeding, the main notations and definitions used in the present article are in order. The notations are provided in Table 1, and the definitions are as follows (Nassar et al., 2021).

Definition 1 (BS-UE Association): BS-UE association is the assignment of a UE to a BS, for establishing a communications channel between the two.

Definition 2 (Association Rule): A UE is always associated with the closest BS in the Euclidean plane. That is, the UE is closer to its associated BS than to any other BS.

Definition 3 (Typical Receiver): The typical receiver is the receiving device (UE or BS) where the SIR is to be assessed. It is always placed at the center of the Euclidean plane in the SG model, or the center of the simulation window of the corresponding simulation model.

Definition 4 (Tagged Transmitter): The tagged transmitter is the transmitting device (UE or BS) that is associated with the typical receiver.

Definition 5 (Typical Circle): The typical circle is the circle centered at the typical receiver with the tagged transmitter on its perimeter.

Definition 6 (Interferer): An interferer is a transmitter that causes interference at the typical receiver. Thus, every transmitter in the network except the tagged transmitter, is an interferer.

Definition 7 (SIR): The Signal to Interference Ratio (SIR) is the quotient of the transmission received at the typical receiver from the tagged transmitter and the sum of the transmissions arriving at that receiver from all interferers in the plane.

As per Definitions 2, if the BS density is λ, it can be shown (Andrews et al., 2023) that the distance *R* between the two elements of a BS-UE pair is a random variable (RV) with Rayleigh distribution and the equation (1) is given as, i.e.

$$f_R(r) = 2\tilde{\lambda} r e^{-\tilde{\lambda} r^2}, \quad (1)$$

Where $\tilde{\lambda} = \pi\lambda$ and $r \geq 0$.

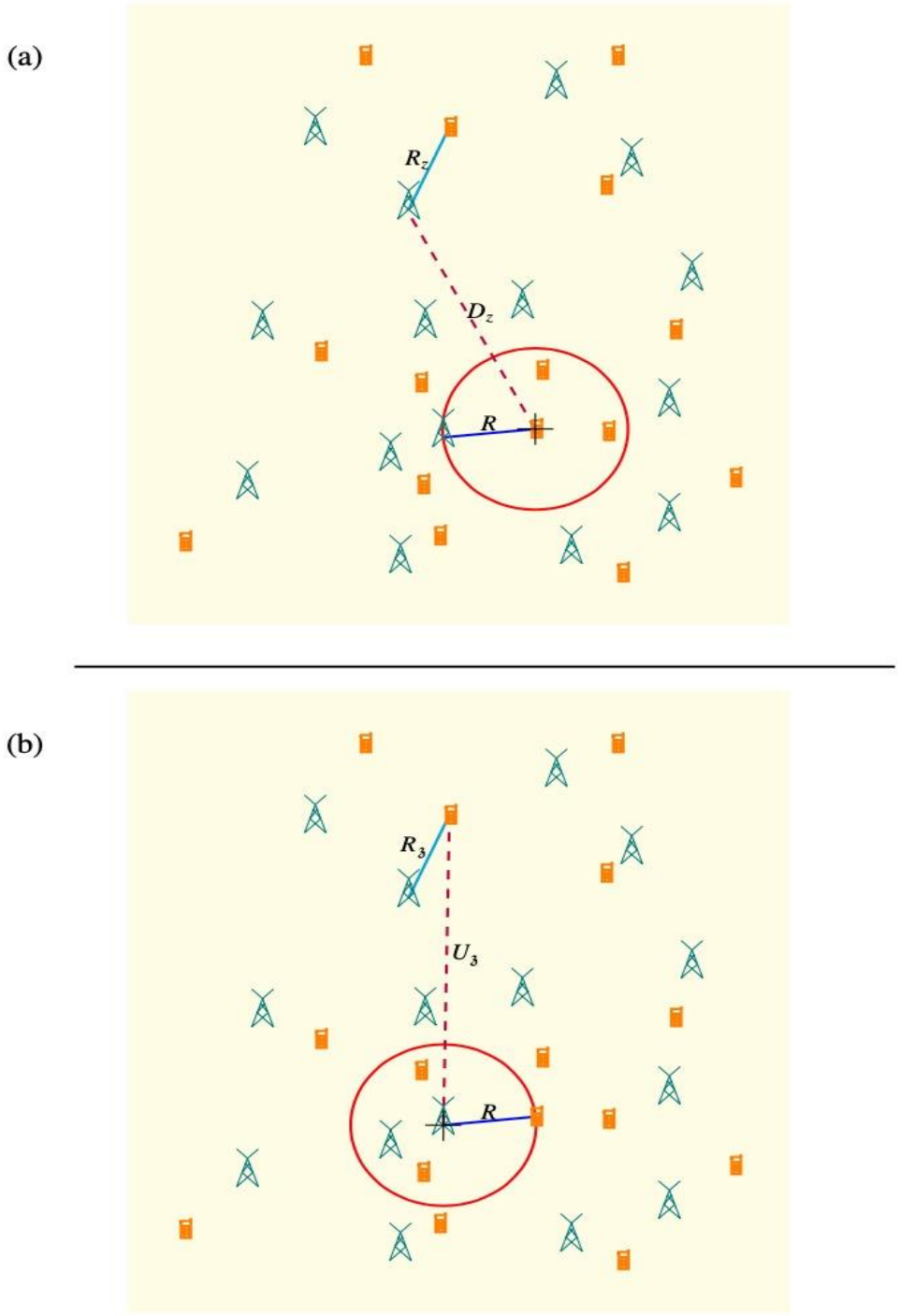

Figure 2: SG Models of a Cellular System for Assessing the SIR at the Typical Receiver. (a) DL model, where the typical receiver is a UE placed at the center of the typical circle. This circle defines an exclusion zone, as it cannot contain a BS. The BSs outside the circle, which cause interference at the typical receiver, form a PPP Φ. (b) UL model, where the typical receiver is a BS placed at the center of the typical circle. This circle does not define an exclusion zone, as it can contain UEs, as shown. The UEs form a PP Ψ, which is not Poisson.

Table 1: Notation Used in SG Model and Simulation

Parameter	Description
Φ	Poisson point process (PPP) of BSs
Φ	Point process of UEs (not Poisson)
λ	Density of BS (per m^2), i.e. intensity of PPP Φ
α	Path-loss exponent (per m), $\kappa = \alpha/2$
SIR	Signal to interference ratio (dB)
ξ	SIR threshold (dB)
G	Rayleigh channel gain of tagged transmitter ($G \sim Exp(1)$)
	Rayleigh channel gain of transmitter i ($G_i \sim Exp(1)$)
$\mathfrak{p}$	BS/UE nominal transmit power (Watts)
ε	Power control factor
p_d	DL coverage probability
p_u	UL coverage probability
N	No. of simulation runs (no. of PPP realizations)
S	Side length of the simulation square window (m)
N	Number of BSs in a simulation run, $N \sim Pois(\lambda S^2)$).
(x,y)	Location of a BS in a simulation run
(u,v)	Location of a UE in a simulation run

We integrate random channel effects by multiplicative RVs, which we denote by G for the tagged transmitter and G_i for each interferer i = 1,2,.... We assume that G and the G_i are independent and identically distributed (iid) following an exponential distribution with average 1 (Andrews et al., 2023). Further, we assume that signals attenuate with distance in accordance with the standard power-law path loss propagation model with exponent $\alpha > 2$. That is, the average power received at distance r from a transmitter of power $\mathfrak{p}$ is $\mathfrak{p}r^{-\alpha}$.

1) Downlink Model

As per Definitions 3 and 4, in the DL model the typical receiver is a UE residing at the origin, and the tagged transmitter is a BS residing on the perimeter of the typical circle of radius R, as shown in Figure 2a. All the BSs outside the typical circle are interferers to the typical UE.

With the above in mind, it can be shown (Nassar et al., 2024) that the DL coverage probability and the equation (2) is given as,

$$p_d = 2\tilde{\lambda}\int_0^\infty e^{-\tilde{\lambda}r^2} e^{-\tilde{\lambda}r^{2\kappa}\sqrt{\xi}\int_{\frac{1}{\sqrt{\xi}}}^{\infty}\frac{1}{1+u^\kappa}du} rdr, \quad (2)$$

Where $\kappa = \alpha/2$.

2) Uplink Model

As per Definitions 3 and 4, in the UL model the typical receiver is a BS residing at the origin, and the tagged transmitter is a UE residing on the perimeter of the typical circle of radius R, as shown in Figure 2b. All the UEs, except the tagged UE, are interferers to the typical BS. That is, the interference at the typical BS is the sum of the signals received at the typical receiver from all the UEs (including those inside the typical circle) in the plane except the tagged UE. While the BSs constitute a PPP Φ of density λ, the UEs constitute another point process Ψ of the same density (as each UE is associated with one and only one BS). However, the process Ψ is not Poisson since its points are not independent, but rather dependent on the points of Φ.

For each UE $\mathfrak{z} \in \Psi$, we denote the distance to its serving BS by $R_{\mathfrak{z}}$ and the distance to the typical BS by $U_{\mathfrak{z}}$. To distinguish it from all other distances, the distance between the tagged UE and the typical BS is denoted by R. As can be seen in Figure 2b, $R_{\mathfrak{z}}$ is upper bounded by $U_{\mathfrak{z}}$ (otherwise the UE at $\mathfrak{z}$ would associate with the typical BS.) Clearly, both R and $R_{\mathfrak{z}}$ are Rayleigh distributed, as they are based on shortest distance associations.

We will consider FPC, whereby each UE $\mathfrak{z}$ adjusts its power level based on its current distance $R_{\mathfrak{z}}$ to the serving BS by a factor is $\varepsilon \in [0, 1]$. Specifically, the transmit power $\mathfrak{p}$ of the UE is amplified by $R_{\mathfrak{z}}^{\varepsilon\alpha}$ to offset the path loss, $R_{\mathfrak{z}}^{-\alpha}$. If $\varepsilon = 0$, there is no offset, which means that the transmit power is invariant to distance, and if it is 1 there is complete channel inversion.

With the above in mind, it can be shown (Nassar et al., 2024) that the UL coverage probability and the equation (3) is given as,

$$p_u = 2\tilde{\lambda} \int_0^{\infty} r e^{-\tilde{\lambda} r^2} e^{-2\tilde{\lambda}^2 \xi r^{2\kappa(1-\varepsilon)} \int_0^{\infty} x \int_0^{x^2} \frac{e^{-\tilde{\lambda} u}}{\xi r^{2\kappa(1-\varepsilon)} + u^{-\varepsilon\kappa} x^{2\kappa}} du dx} dr. \quad (3)$$

4 Simulation Algorithms

In this section, we provide the simulation algorithms we have developed for the above model. Since DL and UL are different, as we have seen in the model above, their simulation algorithms will be introduced separately. We assume that the simulation window, representing the deployment area of the cellular network, is a square of side S m. Then, locations within the simulation window are generated, according to a PPP of intensity λS^2, for the BSs of the network to be simulated (Nassar et al., 2021). At the end of each algorithm, we calculate the SIR at the typical receiver that is placed at the origin.

1) Downlink Algorithm

In DL simulation, after deploying the N BSs in the simulation window, we select the BS closest to the center of the window and make it the tagged BS. We consider that the typical UE is at the center of the window already. Actually, we do not need to generate any UE for simulating the downlink. At the center of the window, where the typical UE is supposed to reside, the transmission received from the tagged BS will be,

Algorithm 1: Simulation of cellular DL system

```
1  Input: 𝒩, ξ, p, λ, S, α
2  Output: p_d
3  Covered := 0
4  for i := 1 to 𝒩 do
       /* Deploy N BSs in simulation window, storing their locations in array D */
5      Generate a Poisson distributed random number N, N~Pois(λS^2)
6      for i := 1 to N do
7          Generate two uniformly distributed coordinates (x, y), x,y~U(−S, S), for BS i.
8          D(i) := (x, y)
9      end
10     Identify tagged BS n, which is the BS nearest the center of the simulation window.
       /* Calculate SIR at typical UE (center of simulation window) and check if it exceeds
          The prescribed ξ : */
11     Generate an exponential random number G, G ~ Exp(1)
12     Calculate distance R between tagged BS and center
13     NUM := pGR^−α
14     DENUM := 0
15     for i := 1 to N do
16         if i ≠ n then
17             Generate an exponential random number G_i, G_i ~ Exp(1)
18             Use array D to calculate the distance D_i between BS i and center
19             DENUM := DENUM + pG_i D_i^−α
20         end
21     end
22     SIR:= NUM/DENUM
23     if SIR > ξ then
           Covered := Covered +1
25     end
   end
       /* Calculate DL coverage probability p_d: */
27     p_d:= Covered / 𝒩
```

Considered signal, whereas the transmissions received from all other BSs will be considered interference. It is a simple matter then to calculate the value of the SIR at the typical UE. If that value exceeds the prescribed SIR threshold ξ, we say that the typical receiver is covered by the tagged transmitter and the 'Covered' variable is incremented. The simulation is run N times, where N is user defined, with each run being a realization. The coverage probability is evaluated after all N runs have been executed, by dividing the number of runs in which the typical UE was covered by the total number N of runs (Mariam et al., 2021).

Now we will analyze the DL algorithm, where the complexity of the algorithm is basically that of one realization. There is a difficulty, however, in analyzing the realization as the number N of BSs there is not constant, but rather a Poisson distributed RV ranging from 0 to ∞. To get around this difficulty, we will use the average number $n = \mathbb{E}[N]$ as a basis for the analysis, where $n = \lambda S^2$. The algorithm, as we can see, is dominated by the lower *for* loop (lines 15–21). This loop is $O(n^2)$, as it has inside a linear search in the association table that contains n entries. Hence, the DL algorithm as a whole is of complexity $O(n^2)$.

2) Uplink Algorithm

In UL simulation, after the BSs have been generated and deployed in the simulation window, the UEs are generated one at a time. Each time a UE is generated, it gets associated to a BS that has not been associated yet. The association criterion is that the UE should be closer to the BS to be associated with than to any other BS in the deployment. If the closest BS is not available, i.e. has already a UE associated with it, then another UE is generated and the criterion is checked again. This procedure is repeated till every BS in the deployment has a UE associated with it.

The data structure that maintains the BS-UE associations is a two-column table, which we call the association table and denote by *A*. The left column is dedicated to *N* BSs and the right for *N* UEs, where *N* is the number of BSs in the deployment. The associations are one-to-one and onto, as demonstrated in the sample Table 2, where each BS or UE is represented by its position in the simulation window. The typical BS, which is placed at the center of the simulation window, with coordinates (0,0), is made the first BS in the table, i.e. BS 1, just for convenience.

Table 2: Example BS-UE Association Table for UL Simulation

BS	**UE**
(0,0)	(-734.2,628.4)
(1243.2, - 221.4)	(973.2,1628.4)
(-345.2,928.4)	NULL
…	…

As seen in the Algorithm, we use in filling the table a novel methodology that accelerates the simulation immensely. Instead of associating the BSs with UEs strictly from the top of the table down, as is traditionally done (Masato et al., 2024), we associate the UE at hand with the closest BS regardless of position of the latter in the table, provided that the BS is available. At the beginning of the algorithm, the right column, which is supposed to hold the UEs, is initialized with NULLs. Then, the left column, which is supposed to hold the BSs, is filled at once by generating *N* pairs of random numbers (drawn from a uniform distribution) in the interval $[-S,S]$, where *S* is the simulation window (square) side. The first number in the pair is the *x* coordinate, and the second the *y* coordinate. Then the UEs are associated with the BSs incrementally, one at a time with no regard to the order of the BS in the table. The association of the first UE is the easiest, since all BSs would be available. The association of the second UE gets a little harder, as one of the BSs would then have become unavailable. The third is even harder, and the last is the hardest.

The association table at the end will store the coordinates of each BS and those of each UE. As such, it can be used to calculate the distance between any BS or UE and any other BS or UE, which we will need when calculating the interference at a given receiver. For example, referring to Table 2, the first BS is at the origin and its associated UE is 734.2 m west and 628.4 m north, i.e. the BS and UE are $\sqrt{734.2^2 + 628.4^2}$= 966.4 m apart. When it is time to associate a UE to a BS, the distances between this UE and all the deployed BSs, whose locations are in the left column, are calculated. The UE is then assigned to the closest of these BSs, if available.

Now we will embark on the asymptotic analysis of the UL algorithm, which is dominated by the filling out of the Association Table *A*. According to our novel methodology of filling out the table, each time a UE is generated, an attempt is made to associate it with *any* of the available BSs, based on the association criterion mentioned above. If this *liberal* criterion is met and if the BS is available, the association is made. Else, the association is not made, but another UE is generated and a fresh association attempt is made for this new UE. This procedure continues as long as there are NULLs in the Table, i.e. there are available BSs that are not associated yet.

That said, each association attempt is basically a Bernoulli trial, ending up in either success or failure. Once one association is made successfully, the probability of success for the next becomes lower, as the number of available BSs will have decreased by 1. Assuming that we have n BSs, the probability of success for the 1st association will be highest, namely 1, whereas that for the last, i.e. nth, will be lowest, namely $1/n$. Specifically, for the kth association, there will be $k-1$ BSs already associated and $n-(k-1)$ BSs available for association. Therefore, the probability of success of the k^{th} association and the equation (4) is given as,

$$\rho_k = \frac{n-(k-1)}{n} \quad (4)$$

Let T_k be the time, i.e. the number of attempts, required until the k^{th} association is made successfully.

Clearly, T_k is geometrically distributed, i.e.

$$\mathbb{P}[T_k = i] = \bar{\rho}_k^{i-1}\rho_k$$
$$= \left(\frac{k-1}{n}\right)^{i-1}\frac{n-k+1}{n}, i = 1,2,\ldots.$$

Accordingly, the expected time to complete the k^{th} association is,

$$\mathbb{E}[T_k] = \frac{1}{\rho_k}$$
$$= \frac{n}{n-k+1}.$$

As a consequence, the expected time to complete all n associations is,

$$\mathbb{E}[T] = \sum_{k=1}^{n}\mathbb{E}[T_k]$$
$$= n(1+\frac{1}{2}+\frac{1}{3}+\ldots+\frac{1}{n}).$$

Algorithm 2: Simulation of cellular UL system

Input: $\mathcal{N}, \xi, \mathfrak{p}, \lambda, S, \alpha, \varepsilon$
Output: p_u
Covered:= 0
for i := 1 to $\mathcal{N}$ **do**
  /* Set up association table A for N BSs (left column) and N UEs (right column), initializing right column with NULLs: */
  for i := 1 to N **do**
    $A(i, 2)$:= NULL
  end
  /* Deploy BSs randomly in simulation window, placing them in left column of A: */
  Generate a Poisson distributed random number N, $N \sim \text{Pois}(\lambda S^2)$
  $A(1, 1) := (0, 0)$ /* Make BS 1 typical. */
  for i := 2 to N **do**
    Generate random location (x,y), where x,y ~ U$(-S, S)$, for BS i.
    $A(i, 1) := (x, y)$
  end
  /* Successively generate UEs, associating each with the closest available BS: */
  while (NULL $\in A$) **do**
    Generate random location (u, v), $u, v \sim \text{U}(-S, S)$, for a UE.
    Calculate distance between UE and every BS i
    Identify BS n, the BS nearest the UE
    if $A(n, 2)$ =NULL **then**
      $A(n, 2) := (u, v)$
      /* Associate UE with BS n if the latter is available. */
    end
  end
  /* Calculate SIR at typical BS: */
  Generate an exponential random number G, $G \sim \text{Exp}(1)$
  Calculate from association table the distance R between typical BS and tagged UE
  NUM:= $\mathfrak{p} G R^{-\alpha(1-\varepsilon)}$
  DENUM:= 0
  for i := 2 to N **do**
    Generate an exponential random number G_i, $G_i \sim \text{Exp}(1)$
    Calculate from association table distance R_i between UE i and serving BS
    Calculate from association table distance U_i between UE i and typical BS
    DENUM = DENUM + $\mathfrak{p}\, G_i R_i^{\alpha\varepsilon} U_i^{-\alpha}$
  end
  SIR:= NUM/DENUM
  if SIR $> \xi$ **then**
    Covered:= Covered + 1
  end
end
p_u:= Covered / $\mathcal{N}$

The finite series in (5) is the harmonic number H_n, which can be approximated by $\ln n + \gamma$, where $\gamma \approx 0.577$ is the Euler–Mascheroni constant (Graham, 1994). It follows that the complexity of the time required to fill up the entire Association Table, using the proposed novel methodology, is $O(n \ln n)$.

To appreciate the impact of our association methodology, we will now show now that it is superior to that of the traditional methodology, used e.g. in (Masato et al., 2024), whose code is available at (Björnson, 2015), where the Association Table is filled up sequentially from the top to the bottom. That is, they start by associating BS 1, then BS 2, all the way down to BS n. It follows that the kth association will necessarily be made with the kth BS, in contrast to our proposed methodology where the kth

association could be made with any of BS as long as it is available. As a consequence, in the traditional methodology the probability of success of the *k*th association will be constant for all association attempts and all BSs. Specifically, $\rho_k = \rho = 1/n$. With T_k still geometric, then $\mathbb{E}[T_k] = n$, leading to $\mathbb{E}[T] = \sum_{k=1}^{n} \mathbb{E}[T_k] = n^2$. This indicates that the complexity of filling up the association table using the traditional methodology is $O(n^2)$ obviously inferior to the $O(n\ln n)$ of the proposed methodology.

Numerical Results

To test their efficiency and correctness, the simulation algorithms above have been coded in the Matlab (R) language as two separate programs, one for DL and the other for UL. The running time took around 1 hr on a Laptop of 8 GB RAM and Core 5 CPU at 2.4 GHz, for 10000 runs. We have used a square simulation window of side S = 3000 m, and a BS density λ = 0.0001 BSs/m^2.

An important coding idea is in order. The pseudocode shown in the two simulation algorithms calculates the coverage probability for only one value of the threshold, ξ. To sketch a smooth curve over a reasonable range of the SIR threshold, as in the figures below, where the range is from −15 dB to 15 dB, we should then run the algorithm N times, with N typically exceeding 3000 for good convergence, for each of the 31 dB values. To save simulation time, however, we did something interesting that yielded the same results faster. Specifically, in each realization, we compared the resulting SIR with all the values of ξ in the range, starting from −15 dB and going upwards, incrementing the variable 'Covered' each time the former exceeds the latter for this particular value of ξ, for which an array, rather than a single variable, is created. Once the former stops exceeding the latter, we quit the comparisons for that realization. This idea reduced the simulation time significantly, yet produced the same results.

The same idea, by the way, applies in UL when using more than one value of the power control factor, ε. Instead of running N realizations for each ε, we use the same realization to get results for as many ε values as desired.

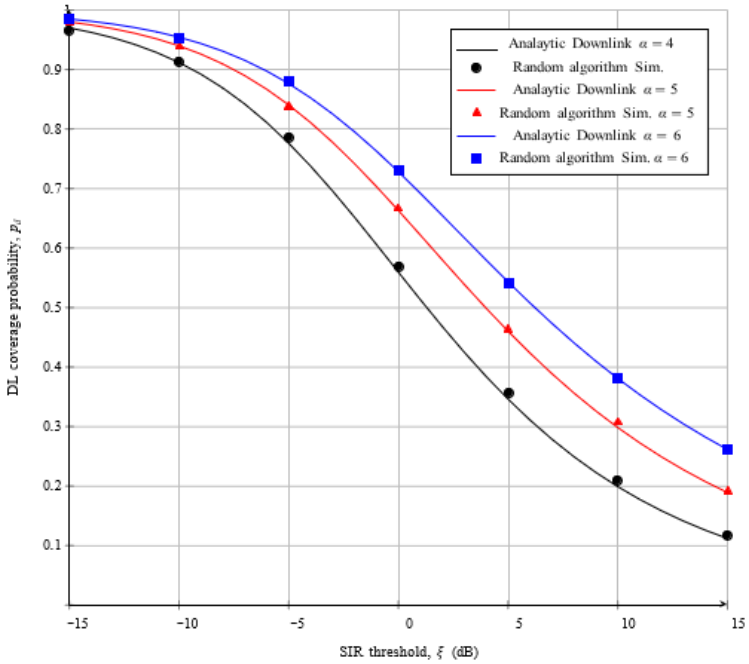

Figure 3: DL Coverage Probability, p_d, Obtained Analytically (Equation (2)) and by Simulation (Square Window Side = 3000 m, λ = 0.0001 BSs/m^2, with $\alpha \in \{4,5,6\}$)

As can be seen, from Figure 3, the simulation results conform impressively with the analytical results, testifying to the correctness of the proposed simulation algorithms. In the three curves shown for $\alpha \in \{4,5,6\}$, the difference between the simulation and analytical results is within 4%. Similarly, from Figure 4, the simulation results conform impressively with the analytical results, testifying to the correctness of the proposed simulation algorithms. In the three curves shown for $\varepsilon \in \{0,0.5,1\}$, all using $\alpha = 4$, the difference between the simulation and analytical results is within 5%. We note in passing that Matlab (R), besides being used for coding the simulation algorithms, was also used to perform the computations of the analytical results. It proved particularly powerful with the numerical computations of the intimidating integrals in (2) and (3) drawn in the Figure.

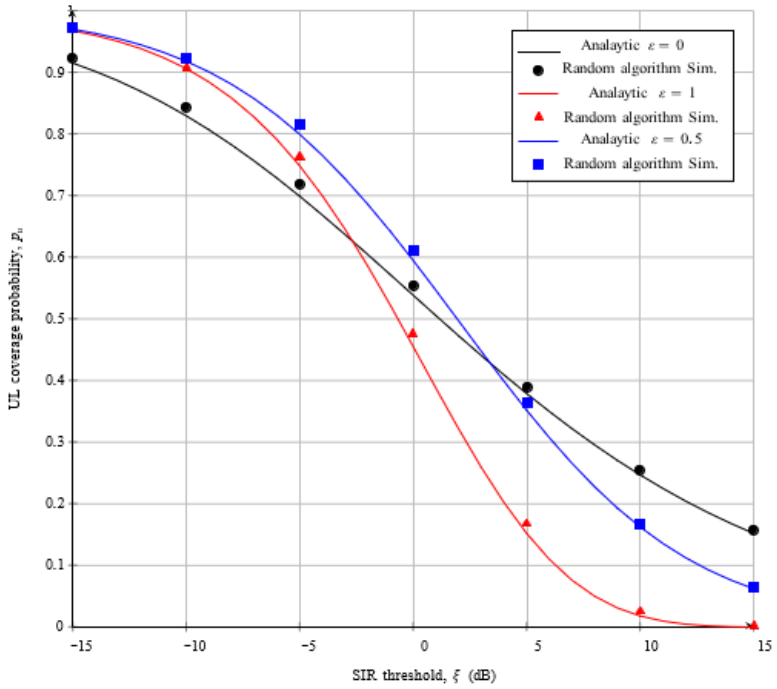

Figure 4: UL Coverage Probability, p_u, Obtained Analytically (Equation (3)) and by Simulation (Square Window Side = 3000 m, $\lambda = 0.0001$ BSs/m^2, $\alpha = 4$, with $\varepsilon \in \{0,0.5,1\}$)

5 Conclusions

In this article we have introduced two Monte Carlo algorithms, Based on SG, to simulate cellular DL and UL communications. The algorithms take as input the parameters of the cellular system and give as output the coverage probability. They start by deploying the BSs as a PPP and the UEs as satellites to the BSs, producing in effect a Voronoi tessellation diagram overlaying the deployment plane. Then they use the system parameters to obtain the SIR at the typical receiver, and from this the coverage probability is obtained. The correctness of the algorithms is proved by comparing their results to the analytical results of the same sample systems. We give implementation ideas that can accelerate the run time immensely. Although the algorithms are designed for a specific cellular model, they can be easily adapted for any other model. In addition, they can be easily adapted for SG applications in fields other than wireless communications, e.g. in biology, material science, forestry and astronomy.

References

[1] Ali, S., Aslam, M. I., & Ahmed, I. (2019). Uplink coverage probability and spectral efficiency for downlink uplink decoupled dense heterogeneous cellular network using multi-slope path loss model. *Telecommunication Systems, 72*(4), 505-516. https://doi.org/10.1007/s11235-019-00587-3.

[2] Amira, M., Mohamed, H. M., & Hamed, N. (2023). Effectiveness of Guard Zone in Mitigating Interference in D2D Underlaid Cellular Networks. *Journal of Wireless Mobile Networks, Ubiquitous Computing, and Dependable Applications, 14*(3), 112-124., https://doi.org/10.58346/JOWUA.2023.I3.021

[3] Andrews, J. G., Gupta, A. K., Alammouri, A., & Dhillon, H. S. (2023). *An introduction to cellular network analysis using stochastic geometry*. Springer International Publishing. https://doi.org/10.1007/978-3-031-29743-4

[4] Arif, M., Wyne, S., & Ahmed, J. (2020). Efficiency analysis of a K-tier clustered HCN using dual connectivity with DUDe access. *AEU-International Journal of Electronics and Communications, 123*, 153291. https://doi.org/10.1016/j.aeue.2020.153291

[5] Björnson, E. (2015). "Github." https://github.com/emilbjornson/maximal-EE/blob/master/simulationFigure5.m/

[6] Björnson, E., Sanguinetti, L., & Kountouris, M. (2016). Deploying dense networks for maximal energy efficiency: Small cells meet massive MIMO. *IEEE Journal on Selected Areas in Communications, 34*(4), 832-847. https://doi.org/10.1109/JSAC.2016.2544498

[7] Błaszczyszyn, B., Haenggi, M., Keeler, P., & Mukherjee, S. (2018). *Stochastic geometry analysis of cellular networks*. Cambridge University Press. https://doi.org/10.1017/9781316677339.

[8] Bouras, C., & Kalogeropoulos, R. (2020). A QoS driven adaptive mechanism for downlink and uplink decoupling in 5G. *Internet of Things, 11*, 100217. https://doi.org/10.1016/j.iot.2020.100217.

[9] Chen, J., & Yuan, C. (2019). Coverage probability and average rate of downlink user-centric wireless cellular networks with composite κ–μ shadowed and lognormal shadowed fading. *IET Communications, 13*(17), 2805-2813. https://doi.org/10.1049/iet-com.2019.0220

[10] Fadoul, M. M. (2020). Modeling multi-tier heterogeneous small cell networks: rate and coverage performance. *Telecommunication Systems, 75*(4), 369-382. https://doi.org/10.1007/s11235-020-00680-y.

[11] Fadoul, M. M. (2020). Rate and coverage analysis in multi-tier heterogeneous network using stochastic geometry approach. *Ad Hoc Networks, 98*, 102038. https://doi.org/10.1016/j.adhoc.2019.102038.

[12] Graham, R. L. (1994). *Concrete mathematics: a foundation for computer science*. Pearson Education India.

[13] Herath, P., Tellambura, C., & Krzymień, W. A. (2018). Coverage probability analysis of three uplink power control schemes: Stochastic geometry approach. *EURASIP Journal on Wireless Communications and Networking*, 1-14. https://doi.org/10.1186/s13638-018-1120-7.

[14] Jia, X., Fan, Q., Xu, W., & Yang, L. (2019). Cross-tier dual-connectivity designs of three-tier hetnets with decoupled uplink/downlink and global coverage performance evaluation. *IEEE Access, 7*, 16816-16836., https://doi.org/10.1109/ACCESS.2019.2895389.

[15] Kamiya, S., Yamamoto, K., Kim, S. L., Nishio, T., & Morikura, M. (2020). SINR Distribution and Scheduling Gain Analysis of Uplink Channel-Adaptive Scheduling. *IEEE Transactions on Wireless Communications, 19*(4), 2321-2335. https://doi.org/10.1109/TWC.2019.2963866.

[16] Kouzayha, N., Dawy, Z., Andrews, J. G., & ElSawy, H. (2017). Joint downlink/uplink RF wake-up solution for IoT over cellular networks. *IEEE Transactions on Wireless Communications, 17*(3), 1574-1588. https://doi.org/10.1109/TWC.2017.2781696.

[17] Kouzayha, N., Elsawy, H., Dahrouj, H., & Al-Naffouri, T. Y. (2021). Meta distribution of downlink SIR for binomial point processes. *IEEE Wireless Communications Letters, 10*(7), 1557-1561. https://doi.org/10.1109/LWC.2021.3074399.

[18] Lei, J., Chen, H., & Zhao, F. (2018). Stochastic geometry analysis of downlink spectral and energy efficiency in ultradense heterogeneous cellular networks. *Mobile Information Systems*, (1), 1684128. https://doi.org/10.1155/2018/1684128.

[19] Li, Z., He, Y., Yi, D., & Lv, J. (2024). Spatiotemporal correlation and joint coverage probability in ultra-dense mobile networks. *Transactions on Emerging Telecommunications Technologies, 35*(1), e4931. https://doi.org/10.1002/ett.4931

[20] Liu, C. H., Shen, Y. H., & Lee, C. H. (2019). Energy-efficient activation and uplink transmission for cellular IoT. *IEEE Internet of Things Journal*, *7*(2), 906-921. https://doi.org/10.1109/JIOT.2019.2946331

[21] Liu, Q., & Zhang, Z. (2020). The analysis of coverage probability, ASE and EE in heterogeneous ultra-dense networks with power control. *Digital Communications and Networks, 6*(4), 524-533. https://doi.org/10.1016/j.dcan.2020.02.002

[22] Liu, Q., Baudais, J. Y., & Mary, P. (2020). A tractable coverage analysis in dynamic downlink cellular networks. *In IEEE 21st International Workshop on Signal Processing Advances in Wireless Communications (SPAWC)*, 1-5. https://doi.org/10.1109/SPAWC48557.2020.9154321

[23] Llopiz-Guerra, K., Daline, U.R., Ronald, M.H., Valia, L.V.M., Jadira, D.R.J.N., Karla, R.S. (2024). Importance of Environmental Education in the Context of Natural Sustainability. *Natural and Engineering Sciences, 9*(1), 57-71.

[24] Mariam, H., Ahmed, I., & Aslam, M. I. (2021). Coverage probability of uplink millimeter wave cellular network with non-homogeneous interferers' point process. *Physical Communication, 45*, 101274. https://doi.org/10.1016/j.phycom.2021.101274

[25] Masato, M., Toshihiro, Y., & Satoru, K. (2024). Effectiveness of MAC Systems based on LSM and their Security Policy Configuration for Protecting IoT Devices. *Journal of Internet Services and Information Security, 14*(3), 293-315.

[26] Megías, D., Kuribayashi, M., Rosales, A., Cabaj, K., & Mazurczyk, W. (2022). Architecture of a fake news detection system combining digital watermarking, signal processing, and machine learning. *Journal of Wireless Mobile Networks, Ubiquitous Computing, and Dependable Applications (JoWUA), 13*(1), 33-55.

[27] Naga, R.M., Balamurugan, P., Nijaguna, G.S., Swarnalatha, K., Lakshmiramana, P., & Edupuganti, M. (2024). Integrated Internet Architecture and Protocol Framework for Peer-to-peer File Sharing in the Internet of Everything (IoE). *Journal of Internet Services and Information Security, 14*(3), 265-274.

[28] Nassar, H., Taher, G., & El Hady, E. (2024). Remarks on a stochastic geometric model for interference-limited cellular communication. *Indonesian Journal of Electrical Engineering and Computer Science, 34*(2), 1376–1388.

[29] Nassar, H., Taher, G., & El-Hady, E. S. (2021). *Cellular coverage probability is independent of base station density under stochastic geometric models*. http://dx.doi.org/10.2139/ssrn.3936557

[30] Nassar, H., Taher, G., & El-Hady, E. S. (2021). *Stochastic geometric modelling and simulation of cellular systems for coverage probability characterization*. arXiv preprint arXiv:2109.14063.

[31] Nidhi, M., Abhijeet, M.H., Akanksha, M., Sushree, S.D. (2024). Automobile Maintenance Prediction Using Integrated Deep Learning and Geographical Information System. *Indian Journal of Information Sources and Services, 14*(2), 109–114. https://doi.org/10.51983/ijiss-2024.14.2.16

[32] Nur, G., Barış, B. N., Levent, B., Sazaklıoğlu, B. S., & Ak, E. (2023). Buser Transcutaneous Electric Nerve Stimulator Device Design. *Natural and Engineering Sciences, 8*(1), 18-30.

[33] Okegbile, S. D., Maharaj, B. T., & Alfa, A. S. (2021). Stochastic geometry approach towards interference management and control in cognitive radio network: A survey. *Computer Communications, 166*, 174-195. https://doi.org/10.1016/j.comcom.2020.12.011
[34] Onireti, O., Zhang, L., Imran, A., & Imran, M. A. (2020). Outage probability in the uplink of multitier millimeter wave cellular networks. *IEEE Systems Journal, 14*(2), 2520-2531. https://doi.org/10.1109/JSYST.2020.2965001.
[35] Priyanka, J., Ramya, M., & Alagappan, M. (2023). IoT Integrated Accelerometer Design and Simulation for Smart Helmets. *Indian Journal of Information Sources and Services, 13*(2), 64–67.
[36] Sadeghabadi, E., Azimi-Abarghouyi, S. M., Makki, B., Nasiri-Kenari, M., & Svensson, T. (2019). Asynchronous downlink massive MIMO networks: A stochastic geometry approach. *IEEE Transactions on Wireless Communications, 19*(1), 579-594. https://doi.org/10.1109/TWC.2019.2946824.
[37] Siddiquee, K. N. E. A., Andersson, K., Moreno Arrebola, F. J., Abedin, M. Z., & Hossain, M. S. (2018). Estimation of signal coverage and localization in wi-fi networks with aodv and olsr. *Journal of Wireless Mobile Networks, Ubiquitous Computing, and Dependable Applications, 9*(3), 11-24.
[38] Talić, Z., & Mešić, M. (2022). Landslide Remediation on Location of Transmission Line Pole SM 134 on DV 110 kV TS TUZLA C. – TS Dubrave. *Archives for Technical Sciences, 1*(26), 33–42.
[39] Tang, X., Xu, X., & Haenggi, M. (2020). Meta distribution of the sir in moving networks. *IEEE Transactions on Communications, 68*(6), 3614-3626. https://doi.org/10.1109/TCOMM.2020.2975996
[40] Wang, X., & Gursoy, M. C. (2019). Coverage analysis for energy-harvesting UAV-assisted mmWave cellular networks. *IEEE Journal on Selected Areas in Communications, 37*(12), 2832-2850. https://doi.org/10.1109/JSAC.2019.2947929

Authors Biography

Gehad Taher, is Teacher Assistance in the Computer Science Department, Suez Canal University, Egypt. She received her B.Sc. and M.Sc. in Computer Science from the same University in 2003 and 2015 respectively. Her research interests include IoT, Wireless Networks, Modeling and Simulation.

El-sayed El-hady, is Assistant Professor in the Basic Science Department, Suez Canal University, Egypt. He received his B.Sc. and M.Sc. in Mathematics from the same University in 2004 and 2010 respectively. He received his Ph.D. in Mathematics from Innsbruck University, Austria in 2016. His research interests include mathematical modeling, functional equations, and stability of (functional, differential, fractional differential) equations.

Hamed Nassar, received the B.Sc. degree in electrical engineering from Ain Shams University, Egypt, in May 1979, and the M.Sc. degree in electrical engineering and the Ph.D. degree in computer engineering from the New Jersey Institute of Technology, USA, in May 1985 and May 1989, respectively. He has been a full professor in the Department of Computer Science, Suez Canal University, Egypt, since 2004. Besides Egypt, he has taught computer science and engineering courses in USA, Lebanon and Saudi Arabia. Dr. Nassar has published numerous articles in in international journals and conferences. His research interests include mathematical modelling of computer and communications systems, cloud computing and machine learning.